Tailoring the properties of hierarchical TS-1 zeolite synthesized from silanized protozeolitic units

D. P. Serrano[a,b], R. Sanz[a], P. Pizarro[a], I. Moreno[a]

[a]Department of Chemical and Energy Technology, ESCET, Universidad Rey Juan Carlos; [b]IMDEA Energía Institute, c/ Tulipán s/n, 28933 Móstoles, Madrid, Spain

e-mail: david.serrano@urjc.es

Published on:

Applied Catalysis A: General 435–436 (2012) 32–42

doi: http://dx.doi.org/10.1016/j.apcata.2012.05.033

Abstract

Hierarchical TS-1 zeolites, characterized by having a secondary porosity within the supermicro/mesopore region (1.5-6 nm), have been synthesized following a procedure based on the silanization of protozeolitic units, which are previously generated by means of a precrystallization step. The silanization agent, phenylaminopropyltrimethoxysilane (PHAPTMS) acts as crystal growth inhibitor, hindering partially the protozeolitic units growth and aggregation during the crystallization treatment. Both the duration of the precrystallization step and the proportion of the organosilane compound added to the synthesis gel have a significant influence on the physicochemical and textural properties of the resultant materials. Thus, the best precrystallization time, leading to the most enhanced textural properties, is comprised between 22-24 hours. Using this time an appropriate balance between the number of protozeolitic units formed and their size is reached. On the other hand, by controlling the organosilane compound proportion added to synthesis gel, the contribution of the secondary porosity can be tailored. Likewise, amounts of organosilane larger than 5 mol% provide to a secondary porous system more uniform in size. The catalytic activity of these materials was evaluated in 1-octene and cyclohexene epoxidation reactions, using tert-butylhydroperoxide (TBHP) as oxidant. The olefin conversion and TOF values reached by hierarchical TS-1 zeolites are remarkably superior to that obtained with the conventional microporous TS-1 zeolite, being higher when the modification degree of the textural properties is more pronounced. These results can be ascribed to the higher accessibility of both TBHP and olefin to the titanium active sites located in the secondary porous system. Likewise, these zeolites exhibit a high oxidant efficiency and total selectivity to epoxide, parameters which are not affected by the presence of the secondary porosity.

Key words: TS-1 zeolite, hierarchical porosity, silanization, epoxidation.

1. Introduction

Zeolitic catalysts offer a broad range of possibilities for performing reactions with high selectivity in the field of organic synthesis. In this sense, the discovery, by Taramasso et al., in 1983 [1], of titanium-silicalite zeolite (TS-1), with the MFI topology, was a breakthrough in heterogeneous catalysis using zeolites, owing to its excellent catalytic features in a large number of selective oxidation reactions under mild conditions [2-6]. This unique activity of TS-1 zeolite is ascribed to the isomorphical substitution of Si atoms by Ti and the hydrophobic character of its surface [7]. However, the small pore size of TS-1 zeolite limits its application to relatively small substrates and oxidants (i.e. H_2O_2) and imposes severe mass transport limitations [8].

Several strategies have been investigated during the last decades in order to overcome these drawbacks, such as the synthesis of Ti-containing zeolites with larger pores (Ti-Beta zeolite) [9] or Ti-containing ordered mesoporous materials (Ti–MCM-41, Ti-SBA-15) [10, 11]. Unfortunately, the last materials suffer from low hydrothermal stability and low intrinsic activity of the Ti sites, which is mainly derived to the amorphous nature of their walls [12].

Molecular transport in zeolites can be also improved by the generation of an additional porosity to that of zeolitic micropores, commonly named as secondary porosity. Depending on the synthesis strategy, this secondary porosity may vary from the supermicropore to the macropore region. Therefore, this innovative kind of materials, known as hierarchical zeolites, combines the typical characteristics of zeolites, such as a crystalline structure and high surface area, with other properties usually related to amorphous materials, such as the presence of larger pores. Thus, the hierarchical structure generation not only may solve the micropore diffusional problems but also may modify the selectivity and improve the catalyst lifetime. For this reason, research concerning the hierarchical zeolites development has largely been extended in the last decade, becoming one of the most promising ways to overcome the diffusion limitations in microporous catalysts [13].

The secondary porosity may be generated by post-synthesis treatments such as dealumination, desilication or detitanation of preformed zeolites [14-16] or by the use of templates. These methods, denoted as *templating methods*, can be classified in three categories according to the nature of the interface established between the zeolite crystals

and the template: *solid templating, supramolecular templating* and *indirect templating* [17]. In the two former cases, the zeolite growth takes place in contact with either a hard template (solid) such as carbon pearls and nanofibers [18], aerogels [19] or biological templates [20, 21] or through supramolecular assembly structures (soft template) such as surfactants [22], laminar precursors [23] and microemulsions [24]. The subsequent removal of the template, usually by calcination, generates the secondary porosity. Through *indirect templating methods*, hierarchical zeolite materials are formed by crystallization of a raw mesoporous templated material [25] or by a controlled deposition of zeolite nanocrystals onto a mesoporous templated material [26].

In this context, our research group has developed a method for the synthesis of hierarchical zeolites based on perturbing the crystal growth by functionalization of protozeolitic units with organosilane compounds. This strategy has been applied to the synthesis of ZSM-5 [27], Beta [28], Mordenite [29] and ZSM-11 [30]. Likewise, Wang et al. employed organofunctionalized polymers to prepare hierarchical ZSM-5 zeolite with small intracrystalline mesopores having an average pore size around 1-2 nm [31] while Ryoo´s group reported the use of large amphiphilic organosilanes to obtain mesoporous ZSM-5 [32] and sodalite [33].

The procedure for the synthesis of hierarchical zeolites based on silanization of protozeolitic units comprised three steps. The first one, the precrystallization step, consists of a low temperature hydrothermal treatment, in which the generation of small protozeolitic units is favoured. Thereafter, an organosilane compound (phenylaminopropyltrimethoxysilane, PHAPTMS) is added over the precrystallized gel. In this silanization step, the organosilane compound reacts with the hydroxyl groups of the external surface in the small zeolitic units, performing as crystal growth inhibitor during the last step of hydrothermal crystallization at high temperature. Finally, both, the structure directing and silanization agents are removed by means of a calcination treatment. The zeolites obtained by this new method are formed by aggregates of ultra-small zeolitic nanounits, and exhibit, additionally to zeolitic micropores, a secondary pore system in the supermicro/mesopore region, which arises from the space initially occupied by the organosilane molecules.

More recently, we have reported the synthesis of hierarchical TS-1 zeolite through silanization of protozeolitic units, employing different starting materials (SiO_2-TiO_2 xerogels and liquid gels [34, 35]). In these works, we probed that the nature of the raw material have a remarkable effect over the final catalyst features, liquid gels being the most suitable for obtaining hierarchical TS-1 zeolites with the best textural properties and catalytic activity. In this work we explore the feasibility to tailor the physicochemical and catalytic properties of the hierarchical TS-1 zeolite according to two main synthesis parameters: the precrystallization time and the silanization agent proportion added to the gel.

2. Experimental Section

2.1. Catalysts preparation

Hierarchical TS-1 zeolites were prepared by modifying the original TS-1 recipe developed by Taramasso et al. based on the use of tetraethylorthosilicate (TEOS, 99 wt%, Alfa) and tetraethylorthotitanate (TEOT, 99 wt%, Alfa) as silica and titanium sources, respectively [1]. In a typical procedure, TEOS and TEOT were properly mixed under stirring at 30°C for 30 minutes, followed by cooling at 0°C for 15 minutes. Then, 1 M tetrapropylammonium hydroxide (TPAOH) aqueous solution was added drop-wise over the previous mixture under vigorous stirring. This reagent was alkali-free synthesized by reaction of tetrapropylammonium bromide (TPABr, 98 wt%, Aldrich) with Ag_2O (99.99 wt%, Alfa). Subsequently, the mixture was heated at 80°C in order to remove the alcohols generated during the hydrolysis. Afterwards, the resulting clear solution, with a molar composition of SiO_2 : 0.0163 TiO_2 : 0.44 TPAOH : 28.5 H_2O, was precrystallized in a reflux system under stirring conditions at 90°C for times varying in the range 16-28 hours. In a further step, the silanization agent, phenylaminopropyltrimethoxisilane (PHAPTMS, 97 wt%, Aldrich), was added to the resultant protozeolitic units solution. The organofunctionalization reaction was performed under stirring at 90°C for 6 hours in a reflux system. The employed amounts of the silanization agent were between 5-15 mol% in regard to the total silica content in the gel. Finally, the crystallization step was carried out in a teflon vessel under autogenous pressure at 170°C for 8 hours using microwave heating radiation. The solid products were recovered by centrifugation, washed several times with distilled water, dried overnight at 110°C and

calcined at 550°C under static air. The hierarchical TS-1 zeolites so obtained were denoted as follows: TS-1 (a h-b%), where "*a*" and "*b*" indicate the precrystallization time (hours) and silanization agent molar percentage, respectively, employed in the preparation of each sample.

For comparison purposes, a conventional TS-1 zeolite was synthesised as reference following the same procedure above described, but omitting the precrystallization and silanization steps. This last sample was designated as TS-1 (0h-0%).

2.2. Characterization

All samples were characterized by conventional techniques in order to determine their main physicochemical properties. Powder X-Ray Diffraction (XRD) patterns were collected employing CuKα radiation on a Philips X'PERT MPD diffractometer. Diffraction data were recorded between 5 - 50°, using a step size of 0.02° and a counting time of 10 s, respectively. Diffuse Reflectance UV-Vis spectra (DR UV-Vis) were obtained in a CARY 500 spectrometer employing $BaSO_4$ as internal standard. Likewise, Fourier Transform Infrared (FT-IR) spectra were recorded in an ATI MATTSON Infinity Series FT-IR, using the KBr pellet technique. The infrarred absorbance intensity was collected from 4000-400 cm^{-1} with 64 scans and a resolution of 4 cm^{-1}. The Ti content of the catalysts was calculated by Inductively Coupled Plasma Atomic Emission Spectroscopy (ICP-AES) by means of a Varian Vista AX system. On the other hand, the organic content of the as-synthesized samples was estimated by elemental analyses performed on a CHNS Elementar Vario EL III analyzer. Transmission Electron Microscopy (TEM) images were recorded using a PHILIPS TECHNAI 20 microscope operating at 200 kV. Thereby, the samples were crushed, dispersed in acetone and deposited on a carbon-coated copper grid. The textural properties of the synthesized materials were determined by adsorption-desorption analysis. Argon adsorption-desorption isotherms were obtained using a Micrometric ASAP 2010 instrument at -186ºC (87.5 K). The samples were evacuated at 300°C under vacuum for 12 hours prior to the analysis. Specific surface areas were calculated through the BET equation, while the cumulative pore volume curves and pore size distributions (PSD) were estimated by applying the NL-DFT method to the Argon adsorption-desorption isotherms, assuming cylindrical pore geometry. This method has been

also applied for determining the relative contribution of micro and mesopores to both surface area and pore volume.

2.3. Catalytic tests

The catalytic properties of the hierarchical TS-1 samples were evaluated by means of olefin epoxidation reactions, using tert-butylhydroperoxide (TBHP, 5.5 M in decane, Fluka) as oxidant. The olefins tested as substrates were 1-octene (98 wt%, Aldrich) and cyclohexene (99 wt%, Aldrich). The reactions were performed in a 100 ml round bottom flask under stirring conditions at 100ºC for 3 hours, in which 30 mmol of olefin (1-octene or cyclohexene), 35 mmol of TBHP and 200 mg of catalyst were put in contact.

The liquid organic reactants and products were quantified by gas chromatography (capillary column 60 m x 0.25 mm, VARIAN FFAP) equipped with a flame ionization detector (FID) using toluene (Sharlab) as internal standard, while TBHP conversions were determined by iodometric titration.

3. Results and discussion

The synthesis of TS-1 zeolites through the silanization of protozeolitic units procedure [34] involves the incorporation of two steps prior to the conventional hydrothermal crystallization treatment at high temperature (170ºC): a) a precrystallization step, consisting in a relatively low temperature (90°C) hydrothermal treatment, with the aim of promoting the generation of protozeolitic units in the synthesis gel and b) anchoring of an organosilane compound (PHAPTMS) to the protozeolitic units through reaction with their surface hydroxyl groups, forming a barrier against their aggregation during the final crystallization step. These two steps may have a remarkable effect in the physicochemical and textural properties of the hierarchical TS-1, especially, in the secondary porosity generation and, therefore, in their catalytic behaviour. For this reason, in order to suitably tailor and control the hierarchical TS-1 properties, the influences of both the precrystallization time and the silanization agent proportion has been investigated in this work.

3.1. Influence of the precrystallization time

The generation of protozeolitic units through the precrystallization stage may have a significant effect on the final properties of the synthesized materials. This step requires conditions that favour the zeolitic nucleation over the crystal growth, such as the employment of low temperatures [36]. Nevertheless, the duration of the precrystallization step could also have an important effect. Thus, if the precrystallization time is too short, the concentration of protozeolitic units in the clear gel would be too small and the silanization agent would anchor just over a reduced number of zeolitic nuclei. However, if the precrytallization time is very long, the protozeolitic units begin to aggregate with each other, leading to particles with large size.

Herein, in order to study the influence of the precrystallization treatment, several hierarchical TS-1 zeolites were synthesized with precrystallization times varying from 16 to 28 hours using a silanization agent concentration of 5 mol%.

The crystallinity of the materials so prepared was evaluated by means of XRD. Figure 1 shows the XRD patterns of the "as-synthesized" hierarchical TS-1 samples and that of the reference zeolite TS-1 (0%-0h). All samples show reflections typical of the MFI structure while no background signals corresponding to an amorphous phase can be detected, this fact denoting a high crystallinity degree. However, at short precrystallization times, lower intensities are recorded in the reflections of hierarchical TS-1 materials when compared to the reference zeolite. This result can be attributed to a reduction in the size of the crystalline domains. On the other hand, the reflection intensities increase as the precrystallization time is longer, indicating a progressive enlargement of the zeolitic units.

DR UV–Vis spectroscopy is widely used for the characterization of titanium-containing zeolites to check the efficient replacement of Si^{4+} by Ti^{4+} cations. The DR UV–Vis spectra of the calcined TS-1 samples are represented in Figure 2. All TS-1 materials exhibit an absorption band at around 210 nm corresponding to the presence of titanium atoms in tetrahedral coordination. However, this band is slightly broader for the hierarchical TS-1 samples. This additional absorption can be attributed to the existence of some highly dispersed penta- or hexa-coordinated titanium species, which is usually caused by a larger hydration of the zeolite titanium sites. Likewise, absorption at 330 nm is not detected in any sample, indicating the absence of extra framework titanium dioxide.

Table 1 summarizes the chemical composition data and the textural properties of the synthesized samples. The titanium concentration, determined by ICP-AES, is very close to 1 %wt in all samples. The seed silanization agent (SSA) content was estimated by HCN elemental analysis of the as-made zeolites prior to calcination, carrying out a mass balance of N and C. The obtained values are close to the theoretical amount added to the synthesis gel (5 mol%), confirming its effective incorporation onto the protozeolitic units surface.

Figure 3 illustrates the Ar adsorption-desorption isotherms of the TS-1 samples. It can be observed that the reference TS-1 zeolite, TS-1 (0h-0%), exhibits a type I isotherm (according to the IUPAC classification), with a sharp transition in the adsorption branch at $P/P_0 < 0.1$ and almost no adsorption at intermediate relative pressures, which agrees well with its microporous structure. The hysteresis loop at $P/P_0 > 0.9$ can be attributed to the interparticle adsorption on the voids formed between the zeolitic particles. Compared with the reference TS-1 zeolite, the hierarchical TS-1 samples synthesized with different precrystallization times exhibit higher Ar adsorption at low and intermediate relative pressures, the hierarchical TS-1 material prepared with a precrystallization time of 24 hours showing the highest Ar adsorption.. These results can be related to the existence of a secondary porosity, located in the supermicro-mesopore region.

The presence of this additional porosity is confirmed by the pore size distribution (PSD) and cumulative pore curves determined by applying the NL-DFT method to Ar isotherms. Figure 4 shows the PDS and cumulative pore curves corresponding to the TS-1 (22h-5%) sample and reference zeolite TS-1 (0h-0%). Both samples exhibit a peak in the PSD at 5.5 Å, which agrees with the pore size of the MFI structure. Additionally, in the pore size distribution corresponding to hierarchical TS-1 sample, several peaks are detected between 10-60 Å, which confirms clearly the presence of a secondary porosity, located in the supermicro/mesopore range.

Table 1 summarizes the textural properties derived from the Ar adsorption analyses, using the BET equation and NL-DFT method. The subscripts ZM and SP make reference to the zeolitic micropores and the secondary porosity systems, respectively. As it can be appreciated, the hierarchical TS-1 samples exhibit enhanced BET specific area, as well as, higher secondary porosity surface than the reference TS-1. It is noteworthy that the samples

prepared with a precrystallization times of 22 and 24 h posses the highest surface areas, showing values of S_{BET} and S_{SP} of 516-557 and 256-255 m^2/g, respectively. Likewise, the sample prepared with a longer precrystallization time, TS-1 (28h-5%), exhibits lower surface areas with a smaller contribution of the secondary porosity. The variation of the textural properties as a function of the precrystallization time can be explained taking into account the crystal growth mechanism occurring during the precrystallization stage.

At short precrystallization times, the number of zeolitic moieties present in the synthesis gel would be very scarce and not sufficiently developed, indicating that there is an induction time for the protozeolitic units generation. In this situation, the silanization agent is reacting with the reduced amount of protozeolitic units. At longer precrystallization times, the protozeolitic units concentration in the synthesis gel grows. However, if the precrystallization time is too long, large zeolitic entities are formed as the crystal growth is favoured over the nucleation process and, consequently, the silanization agent will react with "too large zeolitic entities". According to this, there is an optimum precrystallization time, in which the nucleation and crystal growth rates provide the appropriate balance between the number and size of the protozeolitic units. The highest contribution of the secondary porosity in terms of surface area indicates that the optimum precrystallization time is around 22-24 hours. Moreover, at this point, it was observed that the synthesis gel, which was initially colourless, turned whitish, which could suggest that numerous protozeolitic units have been generated.

2. Influence of seed silanization agent (SSA) amount.

Once it was probed the importance of selecting an appropriate precrystallization time, it was studied the effect of incorporating different amounts of SSA on physicochemical, textural and catalytic properties of the hierarchical zeolites. For that purpose, different hierarchical TS-1 zeolites were synthesized using molar percentages of silanization agent (PHAPTMS) of 5, 8, 12 and 15% in regard to the total silica present in the gel added and using a precrystallization time of 24 hours.

According to the XRD patterns (Figure 5), all the samples are well crystallized, showing the diffraction signals corresponding to the MFI structure while the presence of amorphous phases is not detected. Nevertheless, it can be clearly observed that those reflections

become significantly less intense and broader as the SSA amount added during the synthesis is higher, denoting a progressive decrease in the crystal domain size of the samples.

Figure 6 illustrates the FT-IR analysis corresponding to the samples prepared employing different amounts of PHAPTMS. In these spectra, a sharp band located at around 550 cm^{-1}, characteristic of pentasil-type structure zeolites, is observed. This band corroborates the high crystallinity of the samples previously determined by XRD. However, analogously to the XRD patterns, it can be appreciated that the intensity of such band is lower in those samples prepared from silanized protozeolitic units than in the reference TS-1, indicating the presence of smaller crystallites. The band located at around 960 cm^{-1} is attributed to the vibration of the Si–O–Ti bond or the Si–O bond perturbed by the presence of Ti atom in the framework of TS-1. Many authors consider this band as a clear evidence of the Ti incorporation in the zeolite lattice, taking into account that pure silica and aluminium-containing MFI zeolites do not show any signal at this frequency when titanium is not present in their compositions [37, 38]. On the other hand, a broad absorption band in the wavenumber range of 3200-3600 cm^{-1} can be detected, being commonly associated to the presence of water molecules adsorbed on the surface hydroxyl groups. The intensity of this band is stronger in the hierarchical TS-1 samples than in the conventional zeolite. Thus, hierarchical TS-1 samples present a higher hydrophilic character, caused by the generation of the secondary porosity as this is expected to be covered by silanol groups.

Figure 7 shows the DR-UV Vis spectra corresponding to the hierarchical TS-1 samples prepared with different silanization agent amounts. All of them exhibit a strong band centred at 210 nm, characteristic of the isolated Ti^{4+} atoms in tetrahedral coordination. When the silanization agent amount is increased, this band extends up to wavenumber values of 260-280 nm, denoting the existence of penta and hexa-coordinated Ti species formed by interaction with water molecules. This is a clear indication of changes in the Ti coordination for sites located outside the micropores, as they are in a less confined and more hydrophilic environment. Finally, no absorption can be appreciated at a wavelength around 330 nm, confirming that these samples are free of extra-framework TiO_2.

Table 2 summarizes the SSA concentration for the uncalcined samples as well as the solid yield and titanium content of the final zeolites. In general, the titanium concentration is

very similar for all the hierarchical TS-1 samples, around 1 %wt, and very close to that of the reference TS-1 zeolite. The solid yields of the synthesis are comprised between 54.5% and 64.8%, which are higher than that corresponding to the reference zeolite. This fact can be attributed to the longer synthesis times employed for the preparation of hierarchical TS-1 materials. The sample TS-1 (24h-15%), prepared adding the highest silanization agent amount, exhibit a lower solid yield than the rest of the hierarchical catalysts. This fact can be related to the increase of synthesis gel viscosity produced by the addition of the large silanization agent amount, making difficult to achieve a homogeneous mixture.

On the other hand, it must be highlighted the PHAPTMS content is higher than the theoretical amount introduced into the synthesis gel. This difference becomes higher as the theoretical silanization agent amount employed is increased. This result can be explained taking into account the solid yields exhibited by these samples, which are lower than 65%, indicating that not all the precursor silica species are incorporated into zeolite lattice, while the SSA incorporation degree is complete.

Figure 8 illustrates the Ar adsorption-desorption isotherms measured at -186 ºC (87 K) of the TS-1 samples prepared using different seed silanization agent amounts. It can be observed that the isotherm shape of the hierarchical TS-1 samples is different, exhibiting a quite enhanced argon adsorption compared to that of the reference TS-1 zeolite as the SSA concentration is increased. As it has been described previously, the conventional TS-1 zeolite exhibits a typical type I isotherm, characteristic of microporous materials. However, a gradual transition from the type I isotherm to another having more similar features of type IV isotherms occurs in the hierarchical TS-1 samples as the SSA concentration increases. Thus, argon adsorption at medium/high relative pressures takes place and a hysteresis loop in the same region appears. Both effects, typical of mesoporous materials, are more pronounced as the SSA amount employed in the silanization stage is higher. Consequently, the higher adsorption observed at relative pressures below 0.2 corresponds not only to the presence of the typical MFI microporosity but also to the formation of the Argon monolayer within the mesopores. In conclusion, the generation of an additional pore system in the supermicro/mesopore region is evident, being directly proportional to the SSA concentration employed.

The textural properties of these samples, determined by applying the BET equation and NL-DFT method, are listed in Table 2. It can be appreciated that all hierarchical TS-1 materials exhibit enhanced BET surface areas when compared to the reference TS-1 zeolite. This is due to a clearly superior contribution of the secondary porosity, which increases directly with the SSA concentration employed. Thus, while for the reference TS-1 sample, the BET surface area, secondary porosity surface area (S_{SP}) and secondary pore volume (V_{SP}) are 446 m^2/g, 84 m^2/g and 0.075 cm^3/g, respectively, such parameters are increased up to 693 m^2/g, 479 m^2/g and 0.381 cm^3/g, respectively, for the sample TS-1 (24h-15%). It is important to remark that for this last sample the surface attributed to the secondary porosity represents more than 65% of the total specific surface area. Likewise, it is noteworthy that there is an obvious relationship between the quantity of seed silanization agent added into the synthesis gel and the modification degree of the TS-1 textural properties.

Through the application of the NL-DFT model to the argon adsorption-desorption isotherm, the cumulative pore volume curve and its derivative as a function of the pore size (pore size distribution curve) have been estimated. Figure 9 illustrates both curves determined for the hierarchical TS-1 materials and for the reference zeolite, TS-1 (0h-0%). In regard to the pore size distribution curve, all samples exhibit the expected peak located at 5.5 Å, corresponding to the channel dimensions of the MFI structure. An additional adsorption at pore sizes from 15 to 60 Å occurs for the TS-1 zeolites synthesized through silanization of protozeolitic units, evidencing the presence of the secondary porosity in the supermicro/mesopore region. It is noteworthy that the contribution secondary porosity is increased up when the silanization agent amount introduced into the synthesis gel is higher. Likewise, in the hierarchical TS-1 samples prepared with SSA amounts higher than 5 %mol, the secondary pore size distribution becomes narrower, showing a clear peak centred between 30 and 40 Å, indicating that the mesoporosity is more uniform in size.,

Figure 10 illustrates some representative TEM images corresponding to TS-1 (0h-0%) and TS-1 (24h-8%) samples, denoting that their morphology is completely different. The reference TS-1 sample exhibits well-defined crystals with uniform dimensions (around 200 nm) and regular edges. On the contrary, the sample prepared by silanization of protozeolitic units consists of relatively large (150-200 nm) sponge-like aggregates of much smaller nanounits

(around 10 nm). From these images, it may be deduced that the secondary porosity of the hierarchical TS-1 zeolite corresponds to the voids generated between the nanounits. Interestingly, these really small nanounits are well crystallized, as evidenced by the lattice fringes observed in the TEM images taken at higher magnifications.

3.3. Catalytic activity

The previous physicochemical characterization have revealed that hierarchical TS-1 zeolites are highly crystalline, with most of Ti atoms effectively incorporated in tetrahedral positions into the zeolite framework and exhibiting a secondary pore system in the supermicro/mesopore region, which is expected to facilitate the access of bulky molecules to the active sites. In this sense, the catalytic performance of some selected samples previously characterized was evaluated in 1-octene and cyclohexene epoxidation using tert-butylhydroperoxide (TBHP) as oxidizing agent. Owing to the small pore size of conventional microporous TS-1 zeolites, the use of this kind of organic oxidants, having relatively large dimensions, has been traditionally limited [39]. However, the employment of organic hydroperoxides is interesting as it would enable to carry out reactions in water-free media. This is a very important factor when the presence of water molecules is detrimental for the selectivity towards the target products [40].

Table 3 summarizes the total substrate conversion (1-octene o cyclohexene), turnover frequency (TOF), oxidant efficiency and epoxide selectivity values obtained for the TS-1 samples tested. The results obtained evidence that the porous structure plays an important role in the evolution of the epoxidation reaction. Thus, all the hierarchical TS-1 samples exhibit superior activities for the conversion of both substrates than the conventional microporous TS-1 zeolite, TS-1 (0h-0%), reaching conversion and TOF values several times higher. For example, while the reference TS-1 sample leads to 1-octene and cyclohexene conversion values of 6.7 and 22%, respectively, they increase to 42.1 and 85.3, respectively, for the sample TS-1 (24h-8%). This difference is even higher in terms of the turnover frequency values. On the other hand, it is noteworthy that, in all cases, the selectivity towards the target product (epoxide) was 100% and the oxidant efficiency was higher than 90% for all the catalysts. These results probe the relevant effect of the secondary porosity in the zeolites

obtained from silanized protozeolitic units, since it reduces the steric and diffusional hindrances present in conventional TS-1 zeolite.

4. Conclusions

TS-1 zeolites synthesized from organofunctionalized protozeolitics units exhibit a porous system additionally to the conventional MFI microporous channels, located within the supermicro/mesopore range. These hierarchical TS-1 zeolites show high crystallinity with Ti sites effectively incorporated into the zeolite framework. It has been established that both the precrystallization time and the amount of silanization agent added to the synthesis gel strongly affect the physicochemical properties of the catalysts. Thus, it has been found that there is an optimum precrystallization time, around 24 hours, in which the nucleation and crystal growth rates provide the appropriate balance between the number and size of the protozeolitic units, leading to a better anchoring of the silanization agent. The modification degree of the hierarchical TS-1 materials is clearly related to the silanization agent amount employed in the synthesis. Thus, higher proportions of silanization agent enhance the contribution of the secondary porosity, increasing textural properties values (S_{BET} and S_{SP}) and leading to more uniform mesopore size distribution.

The higher accessibility to the active sites of hierarchical TS-1 zeolites makes them very promising catalysts in epoxidation reactions using bulky organic oxidants, whereas conventional TS-1 zeolites show poor catalytic properties. Specifically in this work, the activity of the hierarchical TS-1 samples was several times higher than that obtained with the conventional microporous TS-1 zeolite when they are tested in the epoxidation of 1-octene and cyclohexene, while preserving a high efficiency in the oxidant use and an epoxide selectivity of 100%.

5. Acknowledgements

We want to thank “Ministerio de Educación y Ciencia” (Spain, project CICYT CTQ2005-09078) for its financial support to this research.

6. References

1. M. Taramasso, G. Perego and B. Notari, US Patent 4 410 501 (1983).
2. M.G. Clerici, G. Bellussi, U. Romano, J. Catal. 129 (1991) 159-167.
3. M.G. Clerici, Appl. Catal. 68 (1991) 249-261.
4. L.J. Davies, P. McMorn, D. Bethell, P.C.B. Page, F. King, F.E. Hankock, G.J. Hutchings, J. Catal. 198 (2001) 319-327.
5. A. Exposito, C. Neri, F. Buonomo, M. Taramasso, U. K. Patent 2116974B (1985).
6. P. Rofia, G. Mantegazza, M. Padovan, G. Petrini, S. Tonti and P. Gervasutti, Stud. Surf. Sci. Catal. 55 (1990) 43-51.
7. P. Ratnasamy, D. Srinivas, H. Knözinger, Adv. Catal. 48 (2004) 1-169.
8. H. Xin, J. Zhao, S. Xu, J. Li, W. Zhang, X. Guo, E. J. M. Eimel, Q. Yang, C. Li. J. Phys. Chem. C 114 (2010) 6553-6555.
9. A. Corma, P. Esteve, A. Martínez, S. Valencia, J. Catal. 152 (1995) 18-24.
10. A. Corma, M.T. Navarro and J. Perez-Pariente, Chem. Commun. (1994) 147-148.
11. P. Wu, T. Tatsumi, T. Komatsu, T. Yashima, Chem. Mater. 14 (2002) 1657-1664.
12. M. Ziolek, Catal. Today 90 (2004) 145-156.
13. Y. Huang, K. Wang, D. Dong, D. Li, M. R. Hill, A. J. Hill, H. Wang, Micropor. Mesopor. Mater. 127 (2010) 167-176.
14. J.C. Groen, J.C. Jansen, J.A. Moulijn, J. Perez-Ramirez, J. Phys. Chem. B 108 (2004) 13062-13065.
15. A.H. Janssen, I. Schmidt, C.J.H. Jacobsen, A.J. Koster, K.P. de Jong, Micropor. Mesopor. Mater. 65 (2003) 59-75.
16. Y. Gao, H. Yoshitake, P. Wu, T. Tatsumi, Micropor. Mesopor. Mater. 70 (2004) 93-101.
17. J. Perez-Ramirez, C.H. Christensen, K. Egeblad, C.H. Christensen, J.C. Groen, Chem. Soc. Rev. 37 (2008) 2530-2542.
18. I. Schmidt, C. Madsen, C.H.J. Jacobsen, Inorganic Chemistry 39 (2000) 22792283.
19. Y. Tao, H. Kanoh, K. Kaneko, J. Am. Chem. Soc. 125 (2003) 6044-6045.
20. M.W, Anderson, S.M. Holmes, N. Hanif, C.S. Cundy, Angew. Chem. Int. Ed. 39 (2000) 2707-2710.

21. A. Dong, Y. Wang, Y. Tang, N. Ren, Y. Zhang, Y .Yue, Z. Gao, Adv. Mater. 14 (2002) 926-929.

22. A. Karlsson, M. Stöcker, R. Schmidt, Micropor. Mesopor. Mater. 27 (1999) 181-182.

23. A. Corma, V. Fornés, S.B. Pergher, Th. L.M. Maesen, J.G. Buglass, Nature (1998) 353-356.

24. S. Lee, D.F. Shantz, Chem. Mater. 17 (2005) 409-417.

25. M.J. Verhoef, P.J. Kooyman, J.C. Van der Waal, M.S. Rigutto, J.A. Peters, H. Van Bekkum Chem. Mater. 13 (2001) 683-687.

26. D. Trong On, S. Kaliaguine, Angew. Chem. Int. Ed. 41 (2002) 1036-1040.

27. D.P. Serrano, J. Aguado, J.M. Escola, J.M. Rodríguez, A. Peral, Chem. Mater. 18 (2006) 2462-2464.

28. J. Aguado, D.P. Serrano, J.M. Rodríguez, Micropor. Mesopor. Mater. 115 (2008) 504-513..

29. J. Aguado, D.P. Serrano, J.M. Escola. A. Peral, J. Anal. Appl. Pyrolysis 85 (2009) 352-358..

30. D.P. Serrano, J. Aguado, J.M. Rodríguez, A. Peral, Stud. Surf. Sci. Catal. 170 (2007) 282-288..

31. H. Wang, T. Pinnavaia, Angew. Chem. Int. Ed. 45 (2006) 7603-7606.

32. M. Choi, H.S. Cho, R. Srivastava, C. Venkatesan, D.H. Choi, R. Ryoo, Nat. Mater. 5 (2006) 718-723.

33. G.V. Shanbhag, M. Choi, J. Kim, R. Ryoo, J. Catal. 264 (2009) 88-92.

34. D.P. Serrano, R. Sanz, P. Pizarro, I. Moreno, Chem. Commun. (2009) 1407-1409.

35. R. Sanz, D.P. Serrano, P. Pizarro, I. Moreno, Chem. Eng. J. 171 (2011) 1428-1438.

36. L. Tosheva, V. Valtech, Chem. Mater. 17 (2005) 2494-2513.

37. X.W. Liu, X.S. Wang, X. W. Guo, G. Li, Catal. Today 93 (2004) 505-509.

38. S.C. Laha, R. Kumar J. Catal. 208 (2002) 339-344.

39. A. Bhaumik and T. Tatsumi, J. Catal. 176 (1998) 305-309.

40. L. Y. Chen, G. K. Chuah, S. Jaenicke, Catal. Lett. 50 (1998) 107-114.

Table 1. Physicochemical properties of hierarchical TS-1 samples prepared with different precrystallization times.

Sample	%Ti (wt%)	%PHAPTMS (mol%)	S_{BET}[a] (m^2/g)	S_{ZM}[a] (m^2/g)	S_{SP}[a] (m^2/g)	V_{ZM}[a] (cm^3/g)	V_{SP}[a] (cm^3/g)
TS-1 (0h-0%)	0.97	-	446	362	84	0.222	0.075
TS-1 (16h-5%)	0.89	5.2	491	251	240	0.161	0.279
TS-1 (22h-5%)	0.97	4.6	516	260	256	0.160	0.229
TS-1 (24h-5%)	1.00	5.4	557	302	255	0.174	0.214
TS-1 (28h-5%)	0.95	5.4	508	315	193	0.193	0.151

[a]Determined by NL-DFT method (cylindrical geometry), ZM: Zeolitic micropores, SP: Secondary porosity.

Table 2. Physicochemical properties and solid yields of TS-1 samples prepared with different SSA agent amounts.

Sample	%Ti (wt. %)	Solid Yield (%)	%PHAPTMS (mol)	S_{BET}[a] (m^2/g)	S_{ZM}[a] (m^2/g)	S_{SP}[a] (m^2/g)	V_{ZM}[a] (cm^3/g)	V_{SP}[a] (cm^3/g)
TS-1 (0h-0%)	0.97	51.8	-	446	362	84	0.222	0.075
TS-1 (24h-5%)	1.00	62.9	5.4	557	302	255	0.185	0.206
TS-1 (24h-8%)	1.09	64.8	11.1	606	258	349	0.158	0.290
TS-1 (24h-12%)	0.95	63.4	17.0	616	230	386	0.141	0.350
TS-1 (24h-15%)	1.12	54.5	22.0	693	214	479	0.131	0.381

[a]Determined by NL-DFT method (cylindrical geometry), ZM: Zeolitic micropores, SP: Secondary porosity.

Table 3. Catalytic properties of TS-1 samples in olefin epoxidation employing TBHP as oxidant.

Sample	S_{SP} (m^2/g)	Substrate conversion (%)	TOF (h^{-1})	TBHP efficiency (%)	Epoxide selectivity (%)
1-octene epoxidation					
TS-1 (0h-0%)	84	6.7	11.9	91.5	100
TS-1 (24h-5%)	255	17.9	35.6	92.9	100
TS-1 (24h-8%)	349	42.1	79.5	96.9	100
TS-1 (24h-12%)	386	36.7	68.6	90.0	100
TS-1 (24h-15%)	479	42.6	64.2	90.4	100
Cyclohexene epoxidation					
TS-1 (0h-0%)	84	22.0	55.0	92.0	100
TS-1 (24h-5%)	255	64.5	157.1	95.3	100
TS-1 (24h-8%)	349	85.3	234.7	91.9	100
TS-1 (24h-12%)	386	83.2	215.3	89.7	100
TS-1 (24h-15%)	479	79.4	173.3	96.8	100

Reaction conditions: 100 °C, 3 h, $(TBHP/olefin)_{MOLAR}$= 1.25, 0.2 g catalyst

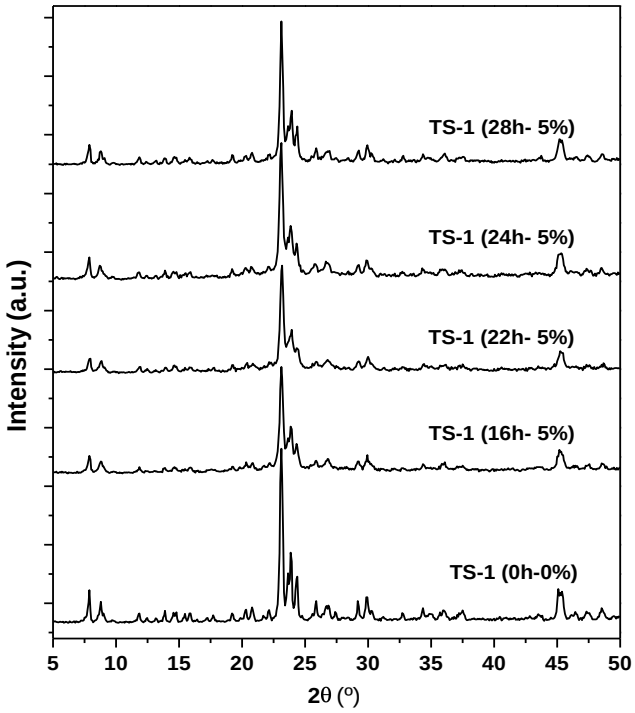

Figure 1. XRD patterns of as-synthesized hierarchical TS-1 samples prepared with different precrystallization times.

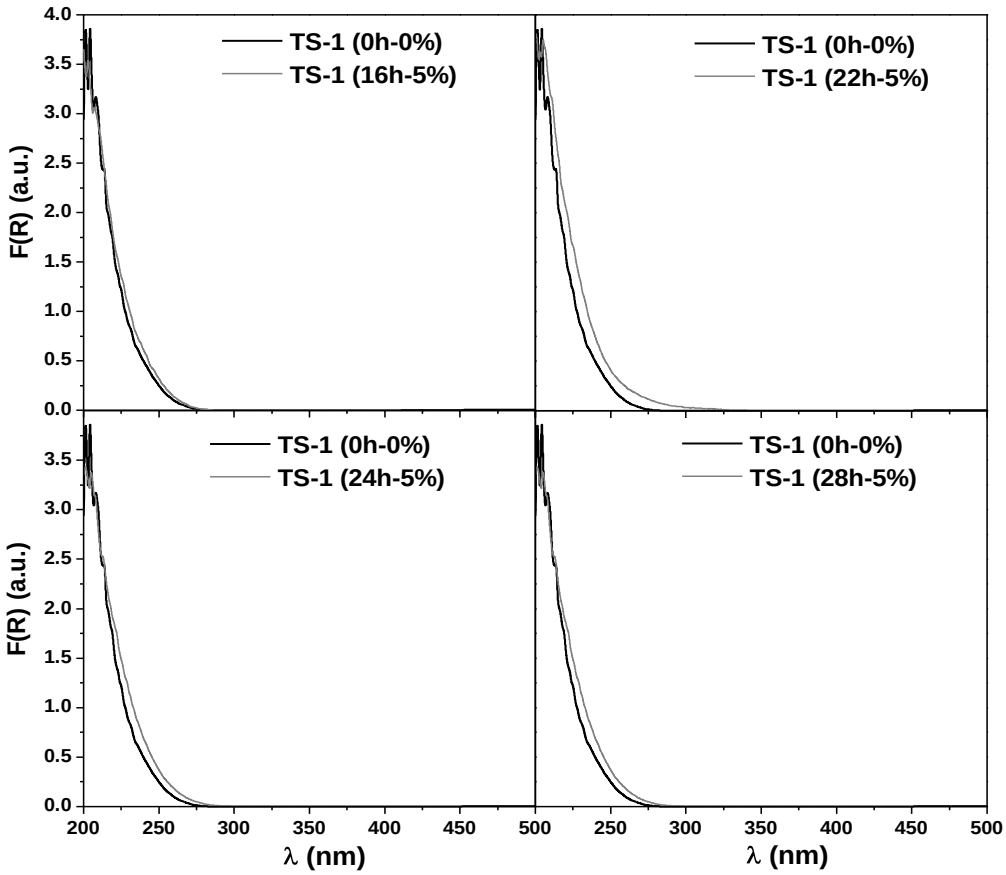

Figure 2. DR UV-Vis spectra of calcined hierarchical TS-1 samples prepared with different precrystallization times.

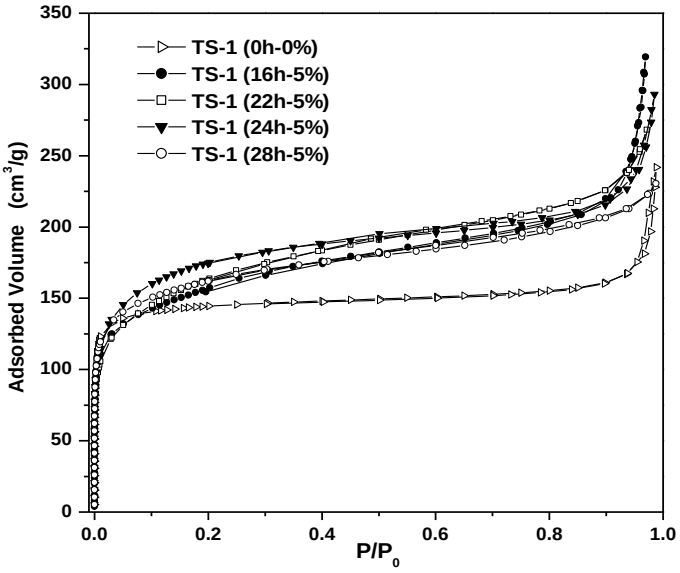

Figure 3. Ar adsorption-desorption isotherms at -186ºC (87 K) of calcined hierarchical TS-1 samples prepared with different precrystallization times.

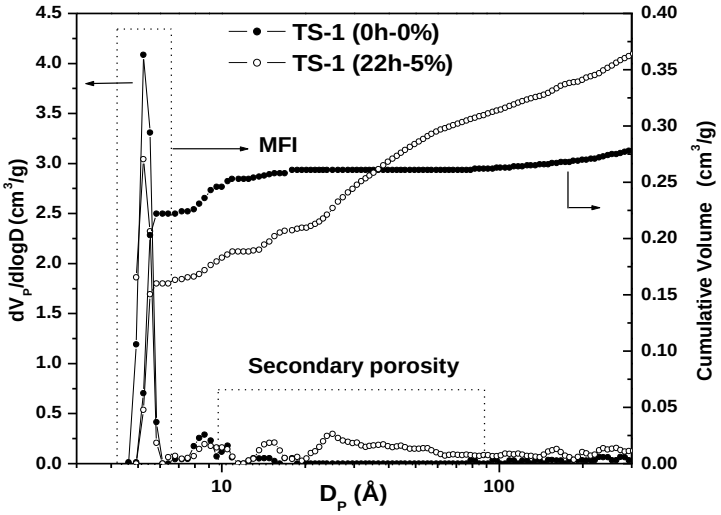

Figure 4. NL-DFT cumulative volume and pore size distribution curves of TS-1 (22h-5%) and TS-1 (0h-0%) samples.

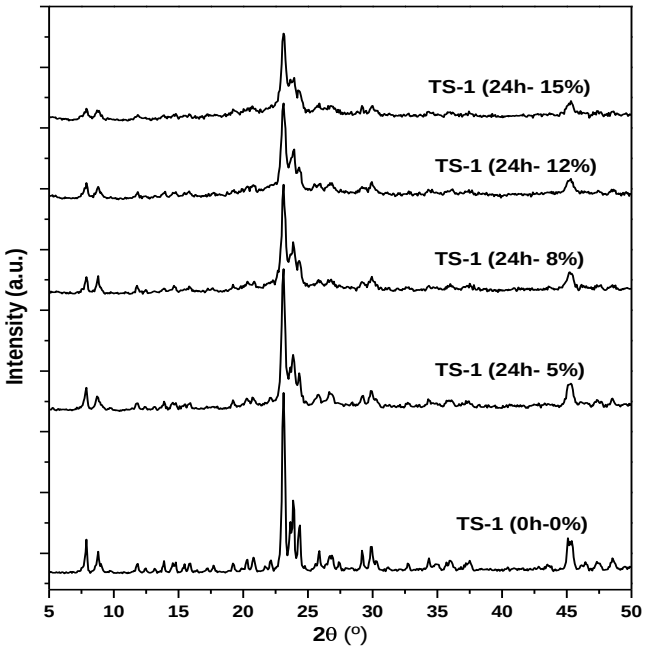

Figure 5. XRD patterns of the as-synthesized hierarchical TS-1 samples prepared with different SSA amounts.

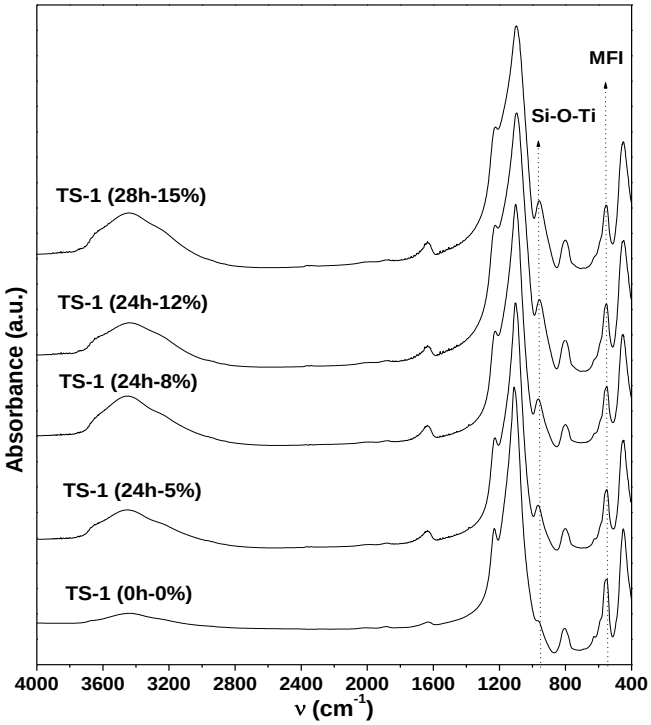

Figure 6. FT-IR analyses of calcined hierarchical TS-1 samples prepared with different SSA agent amounts.

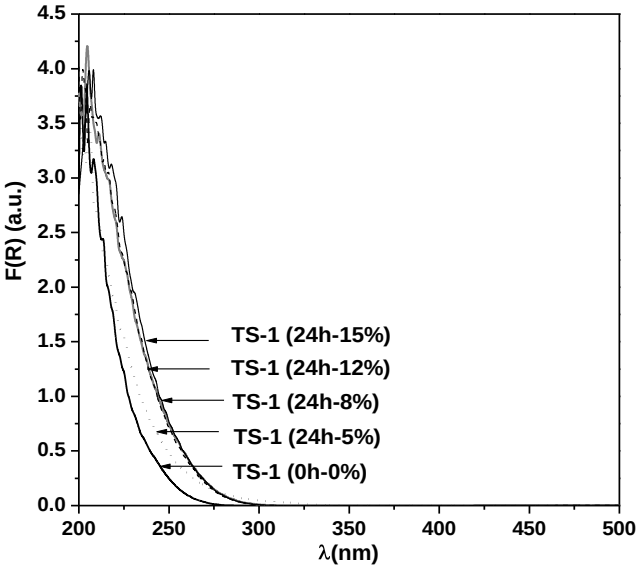

Figure 7. DR UV-Vis spectra of calcined hierarchical TS-1 samples prepared with different SSA agent amounts.

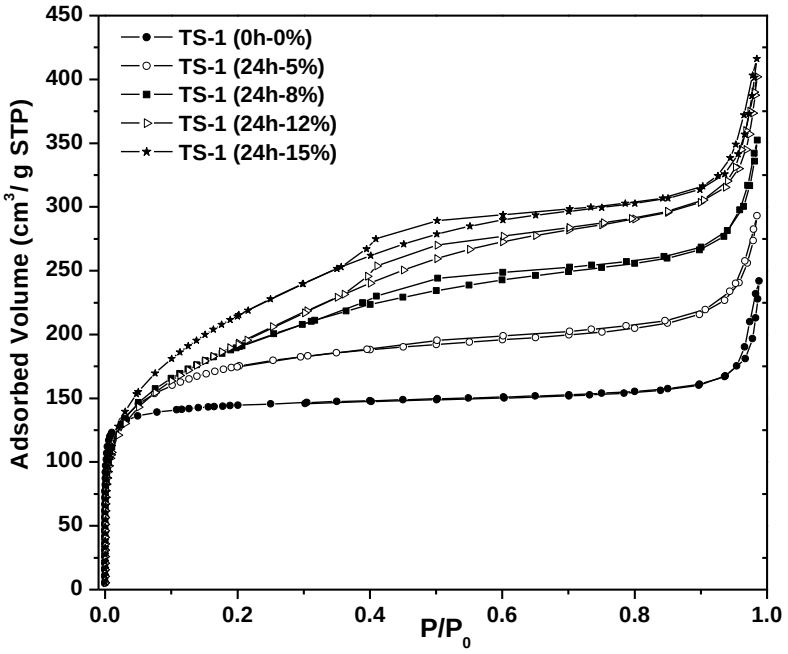

Figure 8. Argon adsorption-desorption isotherms at -186ºC (87 K) of calcined hierarchical TS-1 samples prepared with different SSA agent amounts**.**

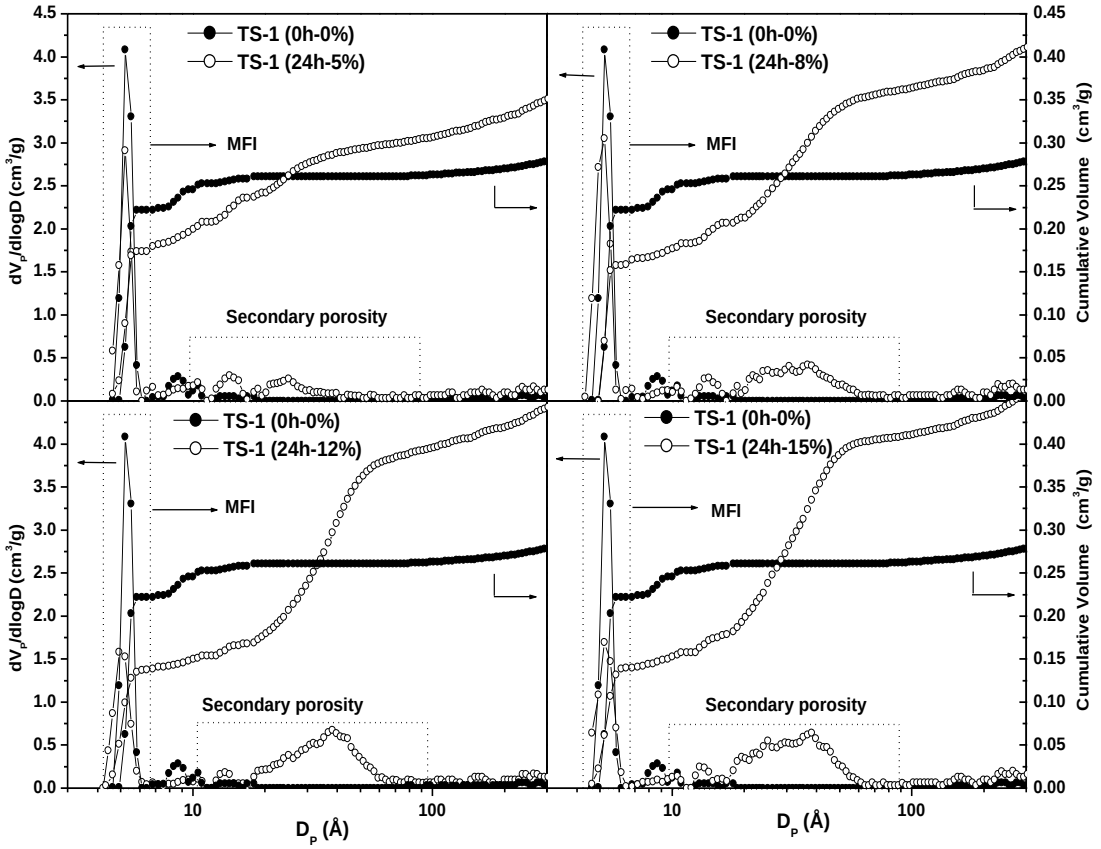

Figure 9. NL-DFT cumulative pore volume and pore size distribution curves of hierarchical TS-1 samples prepared with different SSA agent amounts.

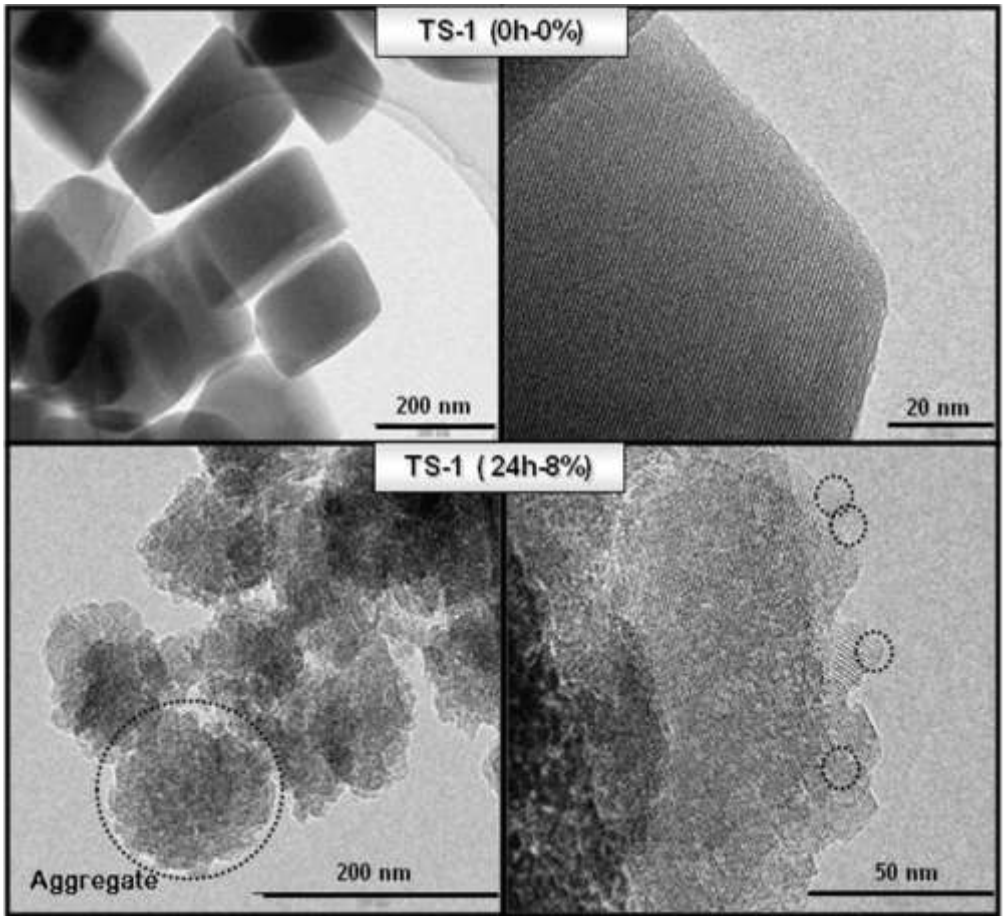

Figure 10. TEM images TS-1 (0h-0%) and TS-1 (24h-8%) samples.